THE JOURNAL OF PHYSICAL CHEMISTRY A

Article

pubs.acs.org/JPCA

Spectral Quasi-Equilibrium Manifold for Chemical Kinetics

Mahdi Kooshkbaghi, Christos E. Frouzakis,* Konstantinos Boulouchos, and Iliya V. Karlin

Aerothermochemistry and Combustion Systems Laboratory, Swiss Federal Institute of Technology, Zurich CH-8092, Switzerland

ABSTRACT: The Spectral Quasi-Equilibrium Manifold (SQEM) method is a model reduction technique for chemical kinetics based on entropy maximization under constraints built by the slowest eigenvectors at equilibrium. The method is revisited here and discussed and validated through the Michaelis−Menten kinetic scheme, and the quality of the reduction is related to the temporal evolution and the gap between eigenvalues. SQEM is then applied to detailed reaction mechanisms for the homogeneous combustion of hydrogen, syngas, and methane mixtures with air in adiabatic constant pressure reactors. The system states computed using SQEM are compared with those obtained by direct integration of the detailed mechanism, and good agreement between the reduced and the detailed descriptions is demonstrated. The SQEM reduced model of hydrogen/air combustion is also compared with another similar technique, the Rate-Controlled Constrained-Equilibrium (RCCE). For the same number of representative variables, SQEM is found to provide a more accurate description.

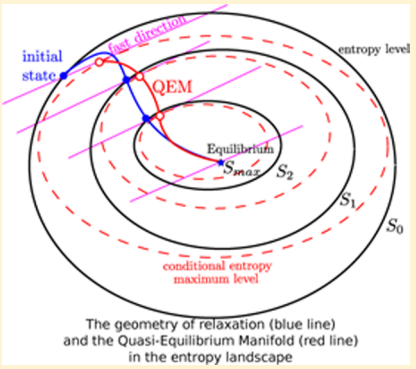

The geometry of relaxation (blue line) and the Quasi-Equilibrium Manifold (red line) in the entropy landscape

1. INTRODUCTION

The macroscopic evolution of complex systems derived from physical and chemical kinetics usually involves variables evolving over a large range of timescales. The disparity of timescales introduces stiffness in the governing equations, and the geometrical structure of the relaxation in the phase space is characterized by trajectories that are rapidly attracted to a hierarchy of submanifolds of lower dimension, and subsequently approach the equilibrium along the Slow Invariant Manifold (SIM).[1] The SIM can be considered as a reliable reduced model of the multiscale dynamics which retains the essential features of the full system with a smaller number of variables and reduced stiffness.

Many different approaches have been proposed for the construction of low-dimensional manifolds for chemical kinetics as described in refs 2−7 and the references therein. In addition to methods that exploit directly the timescale separation, reduction approaches have been developed that are based on thermodynamic functions. Entropy and entropy production are two classical well-studied thermodynamic functions, which can be more informative than the original system dynamics. Entropy can be considered as a Lyapunov function of a closed system and can provide a bridge between thermodynamics and dynamical system analysis. For example, trajectories with minimal entropy production have been considered as candidates for one-dimensional slow manifolds along which the relaxation toward equilibrium mostly proceeds.[8] A one-dimensional slow manifold can be approximated by trajectories of maximal relaxation of the "chemical forces".[9]

Due to timescale disparity, after an initial transient the system dynamics evolves in the vicinity of quasi-equilibrium states (QES), where the entropy is maximized under certain constraints.[10] In chemical kinetics, the Rate-Controlled Constrained-Equilibrium (RCCE) method[11−15] is a quasi-equilibrium based approach which uses the maximum entropy principle and assumes that (i) slow reactions impose constraints on the system evolution, which correspond to slow relaxation toward equilibrium, and (ii) fast reactions equilibrate the system. The system relaxes toward equilibrium through a sequence of constrained-equilibrium states which belong to the Quasi-Equilibrium Manifold (QEM) at a rate controlled by the slowly changing constraints.[2,10]

Originally, chemical intuition guided by numerical simulations was used for the selection of the RCCE constraints,[12] requiring good understanding of the detailed chemical kinetics for finding the class of slow and fast reactions. Other studies tried to determine the species which must be retained in the reduced model based on timescale analysis (e.g Level of Importance[16]), generalizing the parametrization of the RCCE manifold for any comprehensive reaction mechanism.

The majority of fast timescales are exhausted around the equilibrium point; therefore, a low-dimensional SIM is limited around that state. To cover the entire admissible space with a uniform reduced model, one should find a way to extend the manifold. The quasi-equilibrium manifold has been proposed in the literature for species reconstruction (manifold extension) for states far from equilibrium and for determining the manifold boundaries.[17,18]

The spectral quasi-equilibrium manifold (SQEM) uses the left eigenvectors of the Jacobian at equilibrium corresponding to the smallest in absolute value eigenvalues (slowest directions) to construct QEMs. The SQEM has previously been employed only as an initial manifold which was

Received: February 19, 2016
Revised: April 26, 2016
Published: April 26, 2016

DOI: 10.1021/acs.jpca.6b01709
J. Phys. Chem. A 2016, 120, 3406−3413

subsequently refined iteratively toward the SIM.[3,19,20] In this paper, we investigate the potential of the left eigenvectors of the Jacobian at equilibrium employed by the SQEM as a general way to define the quasi-equilibrium constraints without resorting to intuition or detailed understanding of the dynamics under consideration.

The method is first validated using the two-dimensional Michaelis–Menten kinetic scheme, where the quality of the reduction is assessed and related to the temporal evolution and the gap in the spectra of eigenvalues. In addition to simple enzyme kinetics, the potential of the method is explored for detailed combustion mechanisms. The temporal evolution of temperature and the species concentrations deduced from reduced and detailed models are used as indicators of the quality of reduction, showing the potential of SQEM for the reconstruction of species concentrations and temperature profiles. The comparison with the classical RCCE constraints shows that the spectral constraints provide a significantly simpler reduced model which at the considered conditions is in better agreement with the detailed description.

The paper is organized as follows. Reaction kinetics and the SQEM construction formalism as well as an introductory example are presented in Section 2. Validation of the method for realistic fuels follows in Section 3, where the SQEM reduced model is used for the oxidation of hydrogen, syngas, and methane by air in adiabatic isobaric reactors. The main findings are summarized in Section 4.

2. SQEM CONSTRUCTION FOR CHEMICAL KINETICS

2.1. Chemical kinetics. Consider a homogeneous mixture of ideal gases consisting of n_s species and n_e elements at constant pressure p. The molar composition is represented by the vector $\boldsymbol{N} = (N_1, N_2, ..., N_{n_s})^T$ containing the number of moles of the species, and the change in chemical composition is due to a usually complex reaction mechanism represented by r reversible reactions

$$\sum_{i=1}^{n_s} \nu'_{ik} M_i \rightleftharpoons \sum_{i=1}^{n_s} \nu''_{ik} M_i, \qquad k = 1, ..., r \tag{1}$$

Here, ν'_{ik} and ν''_{ik} are the stoichiometric coefficients of species i in reaction k for the reactants and products, respectively. The rate of progress of reaction k is

$$q_k = \underbrace{k_{f_k} \prod_{i=1}^{n_s} [X_i]^{\nu'_{ik}}}_{q_{f_k}} - \underbrace{k_{r_k} \prod_{i=1}^{n_s} [X_i]^{\nu''_{ik}}}_{q_{r_k}}, \qquad k = 1, ..., r \tag{2}$$

where $[X_i]$ denotes the molar concentration of species i and k_{f_k} and k_{r_k} are the forward and reverse rate constants.

Using the reactor volume $\mathbb{V}$ and the rate of progress of reaction k, q_k, the change in the mole number of species in a spatially homogeneous batch reactor i reads

$$\frac{dN_i}{dt} = f(N_i) = \mathbb{V} \sum_{k=1}^{r} (\nu''_{ik} - \nu'_{ik}) q_k, \qquad i = 1, ..., n_s \tag{3}$$

The n_e elemental conservation constraints can be expressed in terms of an $n_e \times n_s$ elemental constraints matrix $\boldsymbol{E}$

$$\mathbf{EN} = \boldsymbol{\xi}^e \tag{4}$$

where the elements of the $\boldsymbol{E}$ matrix, E_{ji}, denote the number of atoms of element j in species i. In closed reactive systems, the elemental mole numbers must be conserved. Hence, $\boldsymbol{EN} = \boldsymbol{\xi}^e$ is fixed upon choosing the fresh mixture, i.e. defining $\boldsymbol{\xi}^e$.

2.2. Equilibrium and quasi-equilibrium. The equilibrium composition, $\boldsymbol{N}^{eq}$, is the constrained minimum of the thermodynamic potential $G(\boldsymbol{N},p,T)$

$$\begin{aligned} &\min \quad G(\mathbf{N}, p, T) \\ &\text{s. t.} \quad \mathbf{EN} = \boldsymbol{\xi}^e \end{aligned} \tag{5}$$

In addition to the elemental conservation constraints (eq 4), the quasi-equilibrium manifold (QEM) imposes n_d additional linear constraints which are regarded as slow macroscopic variables $\boldsymbol{\xi}^d$

$$\mathbf{B}^d\mathbf{N} = \boldsymbol{\xi}^d \tag{6}$$

Here $\boldsymbol{B}^d$ is an $n_d \times n_s$ matrix with rows obtained from the coefficients of the linear combinations of the number of moles providing the n_d slow parameters $\boldsymbol{\xi}^d$. Thus, the total number of constraints in the minimization problem for the quasi-equilibrium amounts to $n_c = n_e + n_d$, and the quasi-equilibrium states which belong to the quasi-equilibrium manifold $\boldsymbol{N}^{QEM}(\boldsymbol{\xi})$ are obtained by solving the following minimization problem

$$\begin{aligned} &\min \quad G(\mathbf{N}, p, T) \\ &\text{s. t.} \quad \mathbf{BN} = \boldsymbol{\xi} \end{aligned} \tag{7}$$

with $\boldsymbol{B} = [\boldsymbol{E};\boldsymbol{B}^d]$ the $n_c \times n_s$ constraint matrix and $\boldsymbol{\xi} = [\boldsymbol{\xi}^e;\boldsymbol{\xi}^d]$ the column vector of constraints with n_c elements; $[;]$ denotes vertical concatenation. The n_s-dimensional state $\boldsymbol{N}$ can then be parametrized by the n_c variables $\boldsymbol{\xi}$. The general form of the constraint matrix $\boldsymbol{B}^d$ reads,

$$\mathbf{B}^d = \begin{bmatrix} \mathbf{v}_1 \\ \vdots \\ \mathbf{v}_{n_d} \end{bmatrix} \tag{8}$$

where $\boldsymbol{v}_i$ is a n_s-dimensional vector defining the ith constraint. It should be noted that the quality of the QEM reduced model depends critically on choosing a good set of constraints.

In the RCCE method, one of the popular realizations of QEM, the constraint vectors $\boldsymbol{v}_i$ correspond to slow reactions controlling the evolution of the chemical composition (for example, three-body dissociation/recombination reactions are imposing slowly varying time-dependent constraints on the total number of moles (TM)[14]). Timescale-based tools have also been used to identify RCCE constraints. Species associated with short timescales can be identified either by the Computational Singular Perturbation radical pointer[21] or by the combined lifetime/sensitivity analysis of the Level of Importance method[16] and ordered in a list according to their fast/slow nature. Usually, the $\boldsymbol{v}_i$ vectors are chosen to point to individual species from the sorted list (i.e., all components of the $\boldsymbol{v}_i$ vector are zero except the one pointing to the chosen species). Slow species are added to the constraints until the comparison between the detailed solution and RCCE manifold shows the desired agreement. Due to the particular form of constraints, RCCE can be formulated as a differential-algebraic problem and has been applied to homogeneous reactors (e.g., refs 13 and 14) and laminar flames.[16,21]

2.3. Spectral quasi-equilibrium manifold. Chiavazzo et al.[3] proposed a different proposed a different set of constraints

DOI: 10.1021/acs.jpca.6b01709
J. Phys. Chem. A 2016, 120, 3406−3413

for the construction of the pertinent quasi-equilibrium based on the left eigenvectors of the Jacobian system at equilibrium

$$J_{ij}^{eq} = \left[\frac{\partial f_i}{\partial N_j}\right]_{\mathbf{N}=\mathbf{N}^{eq}} \tag{9}$$

In this paper, we explore the use of $\boldsymbol{\nu}_{slow}^{eq}$, the left eigenvectors of the Jacobian matrix corresponding to the slowest (nonzero) eigenvalues, as the vectors defining the direction of the slow processes and leading to relaxation toward the final state. In other words, the rows of $\boldsymbol{B}^d$ in eq 8 are the n_d slowest left eigenvectors at equilibrium, excluding the n_e eigenvectors of the zero eigenvalues for elemental conservation. The construction of SQEM is local, meaning that as long as the left eigenvectors at the equilibrium are known, the manifold can be constructed at any point of interest in the phase space. Hence, instead of constructing and tabulating the manifold, the subsequent states of detailed models can be compared with the evolution of the Spectral Quasi-Equilibrium States (SQEs). Before considering the application to detailed combustion mechanisms, the method is illustrated with a simple example.

2.3.1. Reversible Michaelis–Menten mechanism. The Michaelis–Menten (more accurately the Henri–Michaelis–Menten) mechanism is a two-step enzymatic reaction where enzyme E binds to a substrate S to form the intermediate complex ES, which is then converted into the product P, releasing enzyme E.[22] Here, we consider that both reactions are reversible

$$\mathrm{S} + \mathrm{E} \underset{k_{r1}}{\overset{k_{f1}}{\rightleftharpoons}} \mathrm{ES} \underset{k_{r2}}{\overset{k_{\mathrm{cat}}}{\rightleftharpoons}} \mathrm{E} + \mathrm{P} \tag{10}$$

with the rate constants for the forward and reverse reactions denoted as k_{f1}, k_{cat} and k_{r1}, k_{r2}. The temporal evolution of the molar species concentrations $[\mathrm{X}_i]$ is then described by the system of differential equations

$$\frac{d[\mathrm{S}]}{dt} = -k_{f1}[\mathrm{S}][\mathrm{E}] + k_{r1}[\mathrm{ES}] \tag{11a}$$

$$\frac{d[\mathrm{E}]}{dt} = -k_{f1}[\mathrm{S}][\mathrm{E}] + k_{r1}[\mathrm{ES}] + k_{\mathrm{cat}}[\mathrm{ES}] - k_{r2}[\mathrm{E}][\mathrm{P}] \tag{11b}$$

$$\frac{d[\mathrm{ES}]}{dt} = k_{f1}[\mathrm{S}][\mathrm{E}] - k_{r1}[\mathrm{ES}] - k_{\mathrm{cat}}[\mathrm{ES}] + k_{r2}[\mathrm{E}][\mathrm{P}] \tag{11c}$$

$$\frac{d[\mathrm{P}]}{dt} = k_{\mathrm{cat}}[\mathrm{ES}] - k_{r2}[\mathrm{E}][\mathrm{P}] \tag{11d}$$

Due to its simplicity, the model continues to be the focus of numerous studies[23] and a prototypical problem for model reduction. In the absence of an analytic solution, two approaches, the quasi-equilibrium approximation and the steady-state assumption, have been extensively used in the literature to find an expression for the rate of the catalytic step.[24,25] The Michaelis–Menten equilibrium analysis is valid if the substrate reaches equilibrium on a much faster timescale than the product is formed[22]

$$\frac{k_{\mathrm{cat}}}{k_{r1}} \ll 1 \tag{12}$$

The geometric picture of the phase space evolution can be found in refs 26–28, and a comprehensive study of the slow manifold for the Michaelis–Menten mechanism is presented in ref 29.

The system in eq 11 is constrained by two constants for the total enzyme and total substrate concentrations

$$[\mathrm{E}] + [\mathrm{ES}] = \xi_1^e \tag{13a}$$

$$[\mathrm{S}] + [\mathrm{ES}] + [\mathrm{P}] = \xi_2^e \tag{13b}$$

which can be recast in the form of eq 4 with

$$\boldsymbol{E} = \begin{bmatrix} 0 & 1 & 1 & 0 \\ 1 & 0 & 1 & 1 \end{bmatrix}$$

for the concentration vector $\boldsymbol{N} = ([\mathrm{S}], [\mathrm{E}], [\mathrm{ES}], [\mathrm{P}])^T$. The nonlinear system (eq 11) is therefore effectively two-dimensional. The phase portraits for $\xi_1^e = 1.0$, $k_{cat} = 1.0$, and $k_{1f} = k_{1r} = 1$ (Figure 1(a)), $k_{1f} = k_{1r} = 10$ (Figure 1(b)), and $k_{1f} = k_{1r} = 100$ (Figure 1(c)) are given, where the positive semiorbits for different initial conditions are projected on the two-dimensional $[\mathrm{S}] \times [\mathrm{ES}]$ plane. It can be seen that, after short transients, trajectories starting from initial conditions that respect the constraints in eq 13 (dashed lines) are attracted to a slow one-dimensional manifold (thick solid line) and then relax toward the equilibrium point. The slow manifold in Figure 1 is found patch-wise by local integration of the detailed system. For the trajectory initialized with $[\mathrm{ES}]_0 = [\mathrm{P}]_0 = 0$ and $[\mathrm{S}]_0 = 1.0$, discrete time instants are marked for all cases to indicate the evolution time: a decrease in the $\frac{k_{\mathrm{cat}}}{k_{r1}}$ ratio results in faster attraction to the one-dimensional manifold and faster approach of the equilibrium.

Using the rapid equilibrium assumption,[22] the system of ODEs (eq 11a) and (eq 11b) can be integrated in time while the concentration of [ES] can be found by

$$[\mathrm{ES}] = \frac{[\mathrm{E}]_0[\mathrm{S}]}{k_{r1}/k_{f1} + [\mathrm{S}]}$$

The product concentration can be computed from the $[\mathrm{S}] + [\mathrm{ES}] + [\mathrm{P}] = \xi_2^e$ constraint.

Gorban and Shahzad[30] have shown that $G = -\Sigma_{i=1}^{4}[\mathrm{X}_i]\{\ln[\mathrm{X}_i]/[\mathrm{X}_i]^{eq}) - 1\}$ is a Lyapunov function for this mechanism. This functional form has been shown to be a Lyapunov function for homogeneous chemical reaction systems, regardless of whether or not the detailed balance holds at the stationary state.[31]

As discussed in section 2.2, the spectral quasi-equilibrium states for the ODE system (eq 11) can be found by solving the convex optimization problem (eq 7). In this case the constraint matrix is one-dimensional, and it is taken to be equal to the slowest left eigenvector at equilibrium, $[\boldsymbol{B}^d]_{1\times 4} = \boldsymbol{\nu}_{slow}$, so that the 3×4 constraint matrix becomes $[\boldsymbol{B}] = [\boldsymbol{E};\boldsymbol{B}^d]$. For the trajectories starting at $[\mathrm{ES}]_0 = [\mathrm{P}]_0 = 0$ and $[\mathrm{S}]_0 = [\mathrm{E}]_0 = 1.0$, the SQESs are compared with the detailed solutions and the rapid equilibrium assumption results in Figures 2, 3, and 4. The evolution of the eigenvalues, $\boldsymbol{\lambda}$, along the trajectory is also plotted.

For $k_{1f} = k_{1r} = k_{cat} = 1.0$ and $k_{r2} = 10^{-5}$, the slowest left eigenvector at equilibrium is $[\boldsymbol{B}^d] = [0.8507,0,0.5257,0]$ and there is a good agreement between the detailed and reduced systems for the time evolution of the substrate and product (Figure 2(a)) for $t \gtrsim 5$. Far from equilibrium, the SQEM strongly under- or overpredicts the concentrations of [E] and [ES]. The rapid equilibrium results are mostly far away from

DOI: 10.1021/acs.jpca.6b01709
J. Phys. Chem. A 2016, 120, 3406–3413

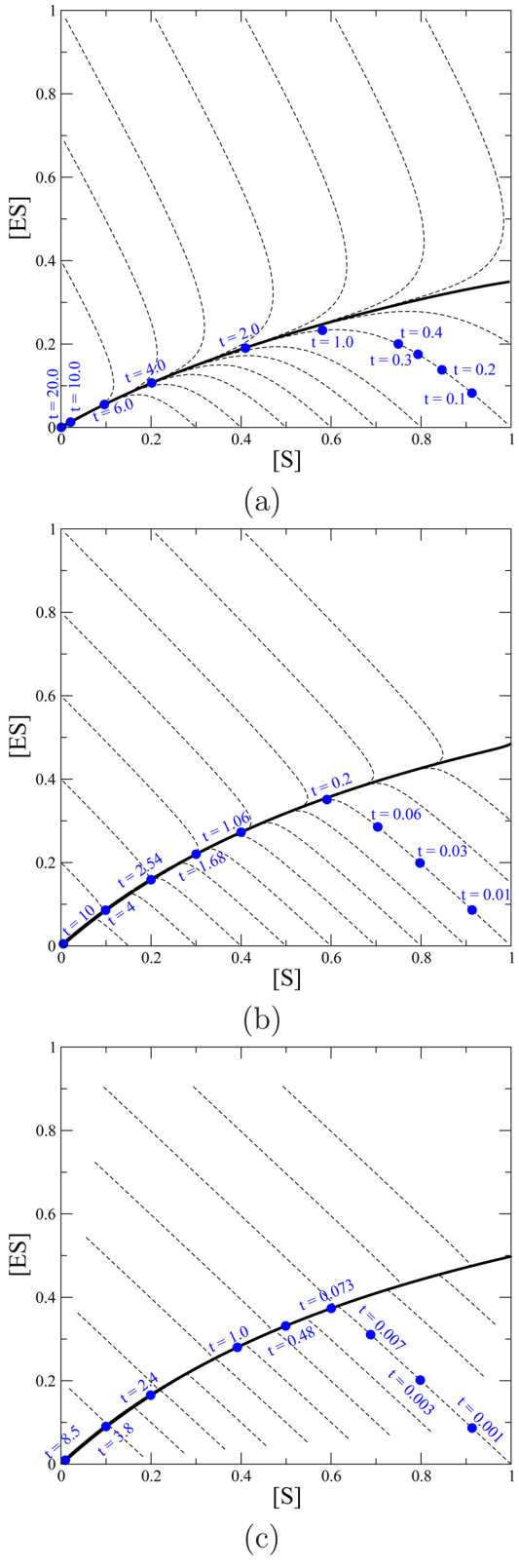

Figure 1. Phase portrait in the [S] × [ES] space for the Michaelis–Menten mechanism with ξ_1^e = 1.0, k_{cat} = 1.0, and $k_{r2} = 10^{-5}$: (a) $k_{1f} = k_{1r}$ = 1, (b) $k_{1f} = k_{1r}$ = 10, (c) $k_{1f} = k_{1r}$ = 100> Dashed line: sample trajectories; solid line: slow manifold; circles mark discrete times for selected trajectories.

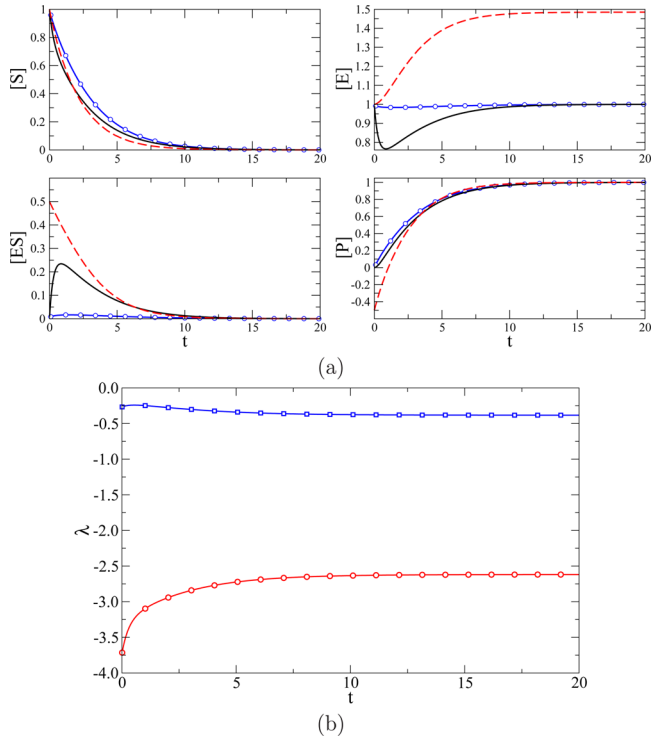

Figure 2. Sample semiorbit for $k_{1f} = k_{1r} = k_{cat}$ = 1.0 and $k_{r2} = 10^{-5}$. (a) Comparison between the profiles of species concentrations computed using the detailed (solid lines), the reduced SQEM description (symbols), and the rapid equilibrium assumption (dashed lines); (b) the evolution of the eigenvalues λ of the system.

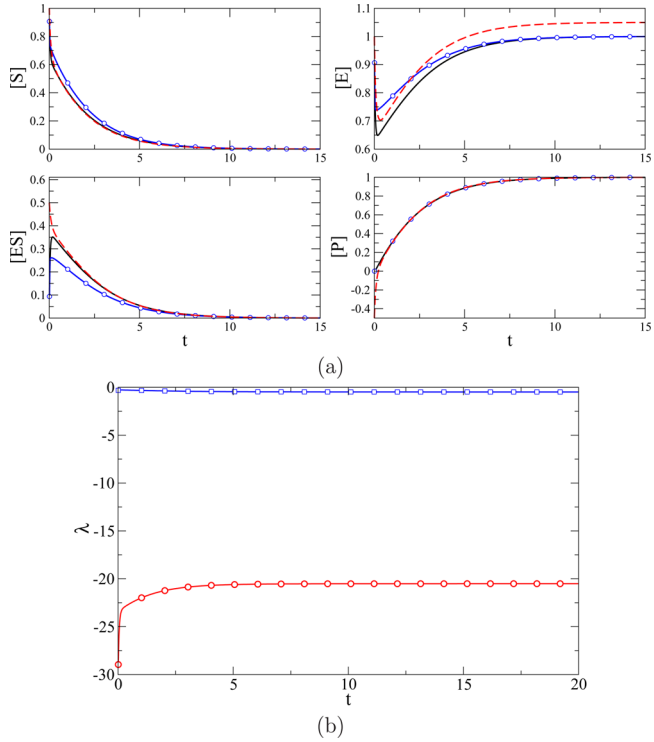

Figure 3. Sample semiorbit for $k_{1f} = k_{1r}$ = 10, k_{cat} = 1.0, and $k_{r2} = 10^{-5}$. (a) Comparison between the profiles of species concentrations computed using the detailed (solid lines), the reduced SQEM description (symbols), and the rapid equilibrium assumption (dashed lines); (b) the evolution of the eigenvalues λ of the system.

DOI: 10.1021/acs.jpca.6b01709
J. Phys. Chem. A 2016, 120, 3406–3413

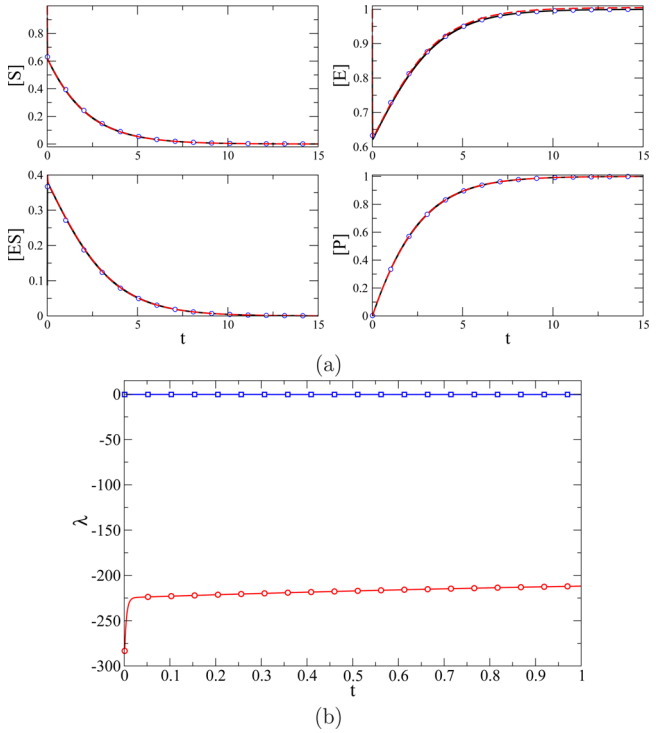

Figure 4. Sample semiorbit for $k_{1f} = k_{1r} = 100$, $k_{cat} = 1.0$, and $k_{r2} = 10^{-5}$. (a) Comparison between the profiles of species concentrations computed using the detailed (solid lines), the reduced SQEM description (symbols), and the rapid equilibrium assumption (dashed lines); (b) the evolution of the eigenvalues λ of the system.

the detailed solution due to the narrow gap between timescales; at equilibrium, the eigenvalue ratio $\lambda_f/\lambda_s \simeq (-2.618)/(-0.382) = 6.85$ is less than one order of magnitude (Figure 2(b)).

The gap between slow and fast processes increases with decreasing ratio $\frac{k_{cat}}{k_{r1}}$, leading to better approximation of the detailed kinetics by the reduced models (Figure 3(a)). For $\frac{k_{cat}}{k_{r1}} = 0.1$ the spectral gap at equilibrium and the slow constraint are $\lambda_f/\lambda_s \simeq 42.0762$ (Figure 3(b)) and $[\boldsymbol{B}^d] = [0.7246,0,0.6892,0]$. The evolution obtained with the reduced description for the [E] and [ES] concentrations is in better agreement with the detailed evolution with respect to the $\frac{k_{cat}}{k_{r1}} = 1$ case, and the SQEM trajectory approaches the detailed one much earlier.

For $\frac{k_{cat}}{k_{r1}} = 0.01$, the agreement between the detailed and reduced formulations for all species is excellent during the whole temporal evolution (Figure 4(a)). The constraint in this case is $[\boldsymbol{B}^d] = [0.7089,0,0.7053,0]$ and the spectral gap is more than two orders of magnitude, $\lambda_f/\lambda_s \simeq 401.96$, resulting in a clear separation of the timescales (Figure 4(b)).

3. COMBUSTION KINETICS

In the following section the potential of the SQEM reduced models is demonstrated for the detailed combustion mechanisms of hydrogen, syngas, and methane corresponding to 6-, 9-, and 27-dimensional systems.

3.1. Autoignition of homogeneous mixtures. In a constant pressure adiabatic system, in addition to the species

Table 1. RCCE Constraint Matrix B^d for the H_2/Air Mixture

Reduced parameter	H_2	N_2	H	O	OH	O_2	H_2O	HO_2	H_2O_2
ξ_1^d = TM	1	1	1	1	1	1	1	1	1
ξ_2^d = AV	0	0	1	2	1	0	0	0	0
ξ_3^d = FO	0	0	0	1	1	0	1	0	0

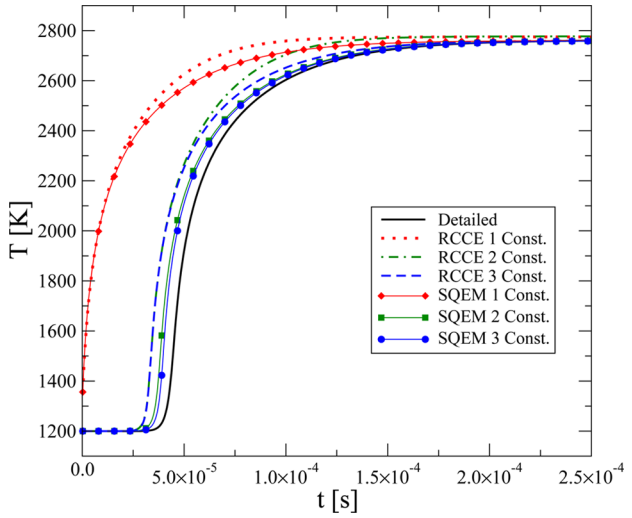

Figure 5. Temperature evolution for stoichiometric H_2/air autoignition under atmospheric pressure with unburnt temperature $T_0 = 1200$ K. The detailed solution is compared with the RCCE and SQEM reduced models with different number of constraints.

production/destruction rates (eq 3), the temperature evolution is governed by

$$\frac{dT}{dt} = -\frac{1}{\rho c_p}\sum_{i=1}^{n_s} h_i \dot{\omega}_i W_i \tag{14}$$

where ρ is the mixture density and W_i, h_i, and $\dot{\omega}_i = \sum_{k=1}^{r} \nu_{ik} q_k$ are the molecular weight, specific enthalpy, and production/destruction rate of species i, respectively. The negative of entropy for ideal gas mixtures under isobaric and isenthalpic conditions takes the form[32]

$$G = -S = -\frac{\sum_{i=1}^{n_s} X_i\left(s_i(T) - R_c \ln(X_i) - R_c \ln\left(\frac{p}{p_{ref}}\right)\right)}{\bar{W}} \tag{15}$$

and $G = -S$ can be considered as the thermodynamic Lyapunov convex function for the dynamics defined by eqs 3 and 14 in terms of s_i, the specific entropy of species i, the mean molecular weight $\bar{W} = \sum_{i=1}^{n_s} X_i W_i$, and the system and reference pressures p and p_{ref}; $X_i = N_i/\sum_{j=1}^{n_s} N_j$ is the mole fraction of species i. Thermodynamic properties and reaction rates were evaluated using CHEMKIN,[33] and the convex minimization problem (eq 7) was solved using the CEQ code,[34] a numerical package for the computation of constrained and unconstrained equilibrium compositions based on the algorithm described in ref 35.

3.1.1. H_2/air mixture results. The detailed kinetic scheme of Li et al.[36] for hydrogen/air mixtures includes $n_s = 9$ species and $r = 21$ reactions. In the scope of RCCE applications for hydrogen combustion, the total number of moles (TM), the total number of radicals referred to as active valence (AV), and free oxygen (FO) have been proposed in refs 12 and 37 as an appropriate set of constraints (Table 1).

DOI: 10.1021/acs.jpca.6b01709
J. Phys. Chem. A 2016, 120, 3406−3413

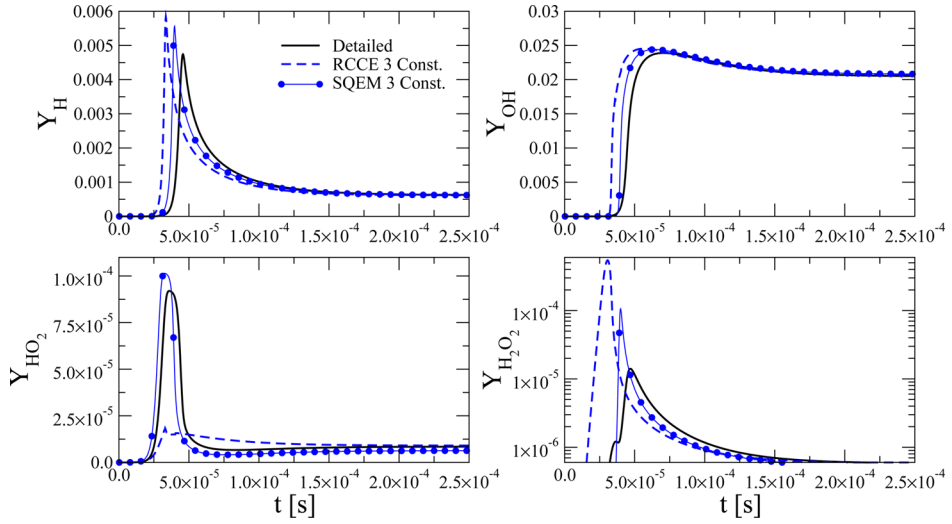

Figure 6. Comparison of the time histories of selected species mass fractions for stoichiometric H_2/air autoignition under atmospheric pressure with initial temperature T_0 = 1200 K computed using the detailed mechanism and with three-dimensional RCCE and SQEM reduced models.

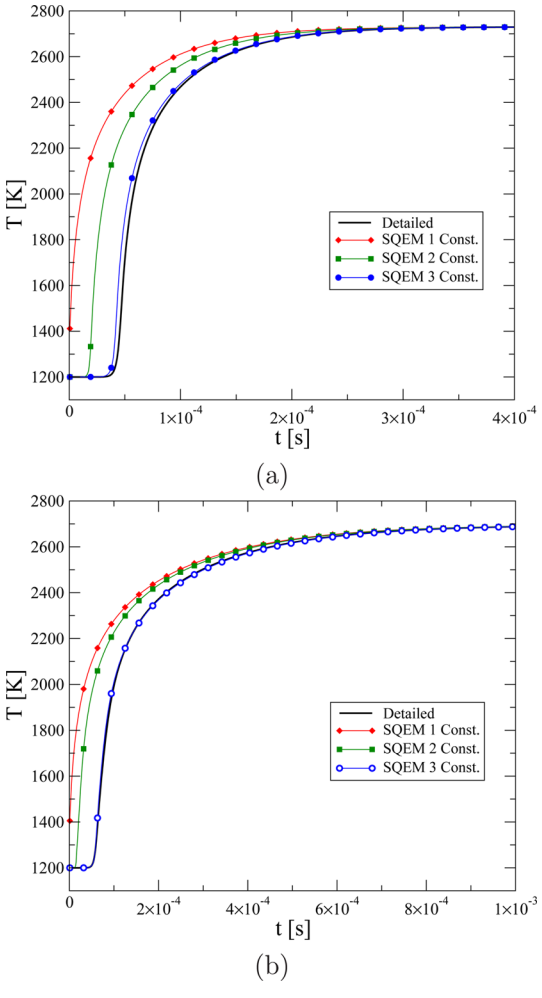

Figure 7. Comparison of the time histories of the temperature evolution for stoichiometric syngas/air autoignition under atmospheric pressure with initial temperature T_0 = 1200 K computed using the detailed mechanism and with SQEM reduced models with different constraints for (a) r_{CO/H_2} = 1/3 and (b) r_{CO/H_2} = 3.

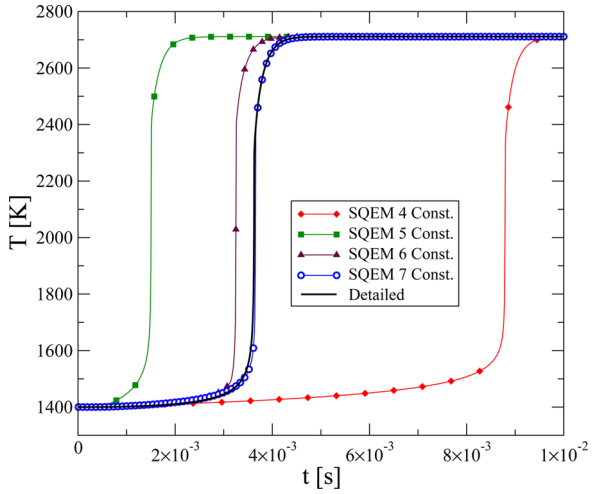

Figure 8. Comparison of the time histories of the temperature evolution for stoichiometric methane/air autoignition under atmospheric pressure with initial temperature T_0 = 1400 K computed using with the detailed mechanism and with the SQEM reduced model with different constraints.

The evolution of temperature for a stoichiometric hydrogen/air mixture at atmospheric pressure with initial temperature T_0 = 1200 K is plotted in Figure 5. The detailed (solid line) solution is compared with SQEM (lines with symbols) and RCCE (dashed, dotted, and dot-dashed lines). It can be seen that, with increasing dimension (number of constraints), the agreement between the reduced and detailed description improves and that for the same dimension the SQEM provides a consistently more accurate description.

In order to obtain a better approximation of the ignition delay time, the initial composition of the constrained-equilibrium state should approximate the actual initial composition.[12] As can be seen in Figure 5, in the one-dimensional case, the initial state is not captured either by SQEM or by RCCE for the constraint based on the slowest left eigenvector and the total number of moles, respectively.

A way to address this issue is to project the initial condition on the one-dimensional manifold. In the classical RCCE which is used here, it is assumed that the rate of change in the unrepresented subspace is negligible and the projector is the identity matrix. Different choices for the projection have been

DOI: 10.1021/acs.jpca.6b01709
J. Phys. Chem. A 2016, 120, 3406−3413

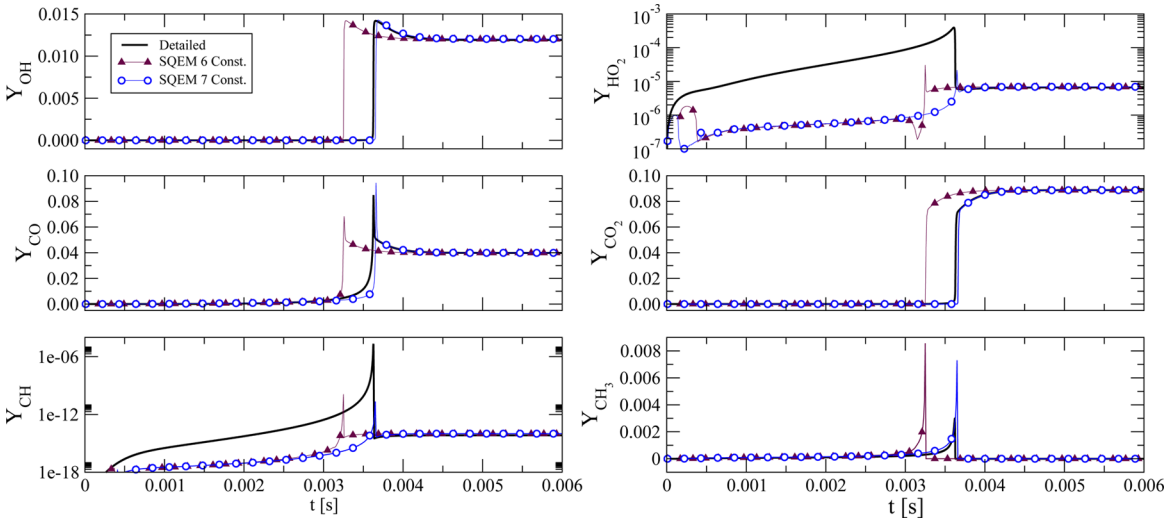

Figure 9. Comparison of the time histories of selected species mass fractions for stoichiometric methane/air autoignition under atmospheric pressure with initial temperature T_0 = 1400 K computed using the detailed mechanism and with SQEM reduced models with different constraints.

introduced in the literature, including the Intrinsic Low Dimensional Manifold,[38] the Computational Singular Perturbation,[39] the thermodynamic projector,[40] and the more accurate projector for RCCE.[37]

The temporal evolution of species mass fractions using three-dimensional reduced QEM models is plotted in Figure 6. SQEM provides a more accurate description even for the low concentration species (hydroperoxy radical HO_2 and hydrogen peroxide H_2O_2).

3.1.2. Syngas/air mixture results. The $CO/H_2/O_2$ elementary scheme of Li et al.[36] was used for the chemistry description with 32 nonduplicate elementary reversible reactions and 13 chemical species. For a stoichiometric mixture of syngas/air in an adiabatic constant pressure (p = 1 atm) reactor at initial temperature T_0 = 1200 K, the temperature evolution captured from the detailed kinetics is compared with that computed using the SQEM reduced descriptions of different dimension. It is shown that, for two $CO:H_2$ molar ratios r_{CO/H_2} = 1:3 and 3:1 (Figure 7 (a) and (b)), the agreement of the SQEM with three constraints and the detailed mechanism for the ignition delay time and the temperature time history are very good.

3.1.3. Methane/air mixture results. The GRI 1.2 mechanism[41] was used to predict the oxidation rates of CH_4. The detailed mechanism includes 31 species and 175 elementary reactions with four elemental conservation constraints for H, O, C, and N; hence, the system is 27-dimensional. The temperature evolution for the stoichiometric mixture with T_0 = 1400 K and p = 1 atm is plotted in Figure 8. The SQEM model with seven constraints captures the temperature profile accurately, implying that the full system in this case can be reduced to a 7-dimensional model. Profiles of selected species found by six- and seven-dimensional SQEM reduced manifolds are compared with the detailed model in Figure 9, exhibiting good agreement for the reduced model with seven constraints.

It should be pointed out that the discrepancy between the reduced and the detailed descriptions reduces nonmonotonically with the dimension of the SQEM model. Similar observations were made in other classes of chemical kinetics model reduction methods based on species elimination techniques.[42,43]

4. CONCLUSION

This paper is devoted to the class of model reduction techniques which are based on the maximization of the entropy function, the Lyapunov function, which increases monotonically along the evolution from an initial condition to the equilibrium state, under specific constraints. The manifold of the conditional maxima of the entropy where the constraints depend on the point on the manifold defines the Quasi-Equilibrium Manifold (QEM). By construction, QEMs are not folded, single-valued, continuous, realizable, and smooth, properties that cannot be guaranteed by other popular reduction methods, such as the Intrinsic Low-Dimensional Manifold (ILDM) method.[6] Furthermore, the QEM construction needs only the entropy function but not the explicit system dynamics (i.e. the exact reaction rates). Since the construction is based on maximization, high-dimensional manifolds can be easily constructed, as shown in the constant pressure autoignition examples considered here, contrary to iterative methods[44] or ILDM. However, the choice of proper constraints plays a vital role in the quality of the reduced model. It is shown that the Spectral Quasi-Equilibrium Manifolds (SQEMs) method, based on the slow left eigenvectors at equilibrium, can be used to define general mathematically-based constraints without resorting to intuition and detailed understanding of the system dynamics to obtain accurate reduced descriptions for combustion kinetics. The autoignition of hydrogen, syngas, and methane shows good agreement of the time histories of the temperature and species concentrations in comparison to detailed models when the number of slow variables is chosen appropriately. The considered cases showed that SQEM can produce more accurate reduced models in comparison to the Rate-Controlled Constrained-Equilibrium (RCCE) approach used in the combustion literature.

Finally, in addition to using the SQEM reduced description directly, the manifold can be iteratively refined to construct slow invariant manifolds (e.g., Method of Invariant Grid[18,19] and the algorithm proposed in ref 44).

AUTHOR INFORMATION

Corresponding Author

*E-mail: frouzakis@lav.mavt.ethz.ch Phone: +41 44 632 79 47.

DOI: 10.1021/acs.jpca.6b01709
J. Phys. Chem. A 2016, 120, 3406−3413

Notes

The authors declare no competing financial interest.

■ ACKNOWLEDGMENTS

Financial support of the Swiss National Science Foundation under Project number 137771 is acknowledged. I.V.K. gratefully acknowledges support by the European Research Council (ERC) Advanced Grant NO. 291094-ELBM.

■ REFERENCES

(1) Jones, C. K. R. T. Geometric Singular Perturbation Theory. *Dynamical Systems* **1995**, *1609*, 44−118.
(2) Gorban, A. N.; Karlin, I. V. Method of Invariant Manifold for Chemical Kinetics. *Chem. Eng. Sci.* **2003**, *58*, 4751−4768.
(3) Chiavazzo, E.; Gorban, A. N.; Karlin, I. V. Comparison of Invariant Manifolds for Model Reduction in Chemical Kinetics. *Commun. Comput. Phys.* **2007**, *2*, 964−992.
(4) Lu, T.; Law, C. K. Toward Accommodating Realistic Fuel Chemistry in Large-Scale Computations. *Prog. Energy Combust. Sci.* **2009**, *35*, 192−215.
(5) Goussis, D. A.; Maas, U. *Turbulence Combustion Modeling*; Springer: 2011; pp 193−220.
(6) Pope, S. B. Small Scales, Many Species and the Manifold Challenges of Turbulent Combustion. *Proc. Combust. Inst.* **2013**, *34*, 1−31.
(7) Turányi, T.; Tomlin, A. *Analysis of Kinetic Reaction Mechanisms*; Springer: 2014.
(8) Lebiedz, D. Computing Minimal Entropy Production Trajectories: An Approach to Model Reduction in Chemical Kinetics. *J. Chem. Phys.* **2004**, *120*, 6890−6897.
(9) Reinhardt, V.; Winckler, M.; Lebiedz, D. Approximation of Slow Attracting Manifolds in Chemical Kinetics by Trajectory-Based Optimization Approaches. *J. Phys. Chem. A* **2008**, *112*, 1712−8.
(10) Gorban, A. N.; Karlin, I. V. *Invariant Manifolds for Physical and Chemical Kinetics*; Springer: 2009.
(11) Keck, J. C.; Gillespie, D. Rate-Controlled Partial-Equilibrium Method for Treating Reacting Gas Mixtures. *Combust. Flame* **1971**, *17*, 237−241.
(12) Law, R.; Metghalchi, M.; Keck, J. C. Rate-Controlled Constrained Equilibrium Calculation of Ignition Delay Times in Hydrogen-Oxygen Mixtures. *Symp. Combust., [Proc.]* **1989**, *22*, 1705−1713.
(13) Keck, J. C. Rate-Controlled Constrained-Equilibrium Theory of Chemical Reactions in Complex Systems. *Prog. Energy Combust. Sci.* **1990**, *16*, 125−154.
(14) Janbozorgi, M.; Ugarte, S.; Metghalchi, H.; Keck, J. C. Combustion Modeling of Mono-Carbon Fuels Using the Rate-Controlled Constrained-Equilibrium Method. *Combust. Flame* **2009**, *156*, 1871−1885.
(15) Beretta, G.; Keck, J.; Janbozorgi, M.; Metghalchi, H. The Rate-Controlled Constrained-Equilibrium Approach to Far-From-Local-Equilibrium Thermodynamics. *Entropy* **2012**, *14*, 92−130.
(16) Rigopoulos, S.; Løvås, T. A LOI-RCCE Methodology for Reducing Chemical Kinetics, with Application to Laminar Premixed Flames. *Proc. Combust. Inst.* **2009**, *32*, 569−576.
(17) Ren, Z.; Pope, S. B.; Vladimirsky, A.; Guckenheimer, J. M. The Invariant Constrained Equilibrium Edge Preimage Curve Method for the Dimension Reduction of Chemical Kinetics. *J. Chem. Phys.* **2006**, *124*, 114111.
(18) Kooshkbaghi, M.; Frouzakis, C. E.; Chiavazzo, E.; Boulouchos, K.; Karlin, I. V. The Global Relaxation Redistribution Method for Reduction of Combustion Kinetics. *J. Chem. Phys.* **2014**, *141*, 044102.
(19) Chiavazzo, E.; Karlin, I. V.; Frouzakis, C. E.; Boulouchos, K. Method of Invariant Grid for Model Reduction of Hydrogen Combustion. *Proc. Combust. Inst.* **2009**, *32*, 519−526.
(20) Shahzad, M.; Rehman, S.; Bibi, R.; Wahab, H. A.; Abdullah, S.; Ahmed, S. Measuring the Complex Behavior of the SO_2 Oxidation Reaction. *Comput. Ecol. Softw.* **2015**, *5*, 254−270.
(21) Jones, W. P.; Rigopoulos, S. Rate-Controlled Constrained Equilibrium: Formulation and Application to Nonpremixed Laminar Flames. *Combust. Flame* **2005**, *142*, 223−234.
(22) Keener, J.; James, S. *Mathematical Physiology*; Interdisciplinary Applied Mathematics; Springer-Verlag: New York, 1998; Vol. *8*.
(23) Cornish-Bowden, A. One Hundred Years of Michaelis-Menten Kinetics. *Perspect. Sci.* **2015**, *4*, 3−9.
(24) Henri, V. Théorie Générale de L'action de Quelques Diastases. *C. R. Acad. Sci. Paris* **1902**, *135*, 916−919.
(25) Briggs, G. E.; Haldane, J. B. S. A Note on the Kinetics of Enzyme Action. *Biochem. J.* **1925**, *19*, 338−339.
(26) Darvey, I. G.; Matlak, R. F. An Investigation of Basic Assumption in Enzyme Kinetics Using Results of the Geometric Theory of Differential Equations. *Bull. Math. Biophys.* **1967**, *29*, 335−341.
(27) Nguyen, A. H.; Fraser, S. J. Geometrical Picture of Reaction in Enzyme Kinetics. *J. Chem. Phys.* **1989**, *91*, 186.
(28) Roussel, M. R.; Tang, T. The Functional Equation Truncation Method for Approximating Slow Invariant Manifolds: a Rapid Method for Computing Intrinsic Low-Dimensional Manifolds. *J. Chem. Phys.* **2006**, *125*, 214103.
(29) Calder, M. S.; Siegel, D. Properties of The Michaelis-Menten Mechanism in Phase Space. *J. Math. Anal. Appl.* **2008**, *339*, 1044−1064.
(30) Gorban, A. N.; Shahzad, M. The Michaelis-Menten-Stueckelberg Theorem. *Entropy* **2011**, *13*, 966−1019.
(31) Shear, D. An Analog of the Boltzmann H-Theorem (a Lyapunov Function) for Systems of Coupled Chemical Reactions. *J. Theor. Biol.* **1967**, *16*, 212−228.
(32) Chiavazzo, E.; Karlin, I. V. Adaptive Simplification of Complex Multiscale Systems. *Phys. Rev. E - Stat. Nonlinear, Soft Matter Phys.* **2011**, *83*, 036706.
(33) Kee, R. J.; Dixon-Lewis, G.; Warnatz, J.; Coltrin, M. E.; Miller, J. A. *Chemkin-III: a FORTRAN Chemical Kinetics Package for the Analysis of Gas-Phase Chemical and Plasma Kinetics*; 1996; Vol. *SAND96*.
(34) Pope, S. B. *Computation of Constrained and Unconstrained Equilibrium Compositions of Ideal Gas Mixtures Using Gibbs Function Continuation* **2003**.
(35) Pope, S. B. Gibbs Function Continuation for the Stable Computation of Chemical Equilibrium. *Combust. Flame* **2004**, *139*, 222−226.
(36) Li, J.; Zhao, Z.; Kazakov, A.; Dryer, F. L. An Updated Comprehensive Kinetic Model of Hydrogen Combustion. *Int. J. Chem. Kinet.* **2004**, *36*, 566−575.
(37) Tang, Q.; Pope, S. B. A More Accurate Projection in the Rate-Controlled Constrained-Equilibrium Method for Dimension Reduction of Combustion Chemistry. *Combust. Theory Modell.* **2004**, *8*, 255−279.
(38) Maas, U.; Pope, S. Simplifying Chemical Kinetics: Intrinsic Low-Dimensional Manifolds in Composition Space. *Combust. Flame* **1992**, *88*, 239−264.
(39) Lam, S. H.; Goussis, D. A. Understanding Complex Chemical Kinetics with Computational Singular Perturbation. *Symp. Combust., [Proc.]* **1989**, *22*, 931−941.
(40) Gorban, A. N.; Karlin, I. V. Thermodynamic Parameterization. *Phys. A* **1992**, *190*, 393−404.
(41) Gregory, P. S.; Golden, D. M.; Frenklach, M.; Moriarty, N. W.; Eiteneer, B.; Goldenberg, M.; Bowman, C. T.; Hanson, R. K.; Song, S.; Gardiner, W. C. et al. *GRI-Mech 1.2*. 1994; http://www.me.berkeley.edu/gri_mech/, visited on 2016−04−26.
(42) Tosatto, L.; Bennett, B. A. V.; Smooke, M. D. Comparison of Different DRG-Based Methods for the Skeletal Reduction of JP-8 Surrogate Mechanisms. *Combust. Flame* **2013**, *160*, 1572−1582.
(43) Kooshkbaghi, M.; Frouzakis, C. E.; Boulouchos, K.; Karlin, I. V. Entropy Production Analysis for Mechanism Reduction. *Combust. Flame* **2014**, *161*, 1507−1515.
(44) Roussel, M. R.; Fraser, S. J. On the Geometry of Transient Relaxation. *J. Chem. Phys.* **1991**, *94*, 7106−7113.

DOI: 10.1021/acs.jpca.6b01709
J. Phys. Chem. A 2016, 120, 3406−3413